

A Granger-Causal Perspective on Gradient Descent with Application to Pruning

Aditya Shah

Google Search, Google Austin, Texas, USA

ADITYSHA@GOOGLE.COM

Aditya Challa

APPCAIR and CS&IS, BITS Pilani KK Birla Goa Campus, India

ADITYAC@GOA.BITS-PILANI.AC.IN

Sravan Danda

APPCAIR and CS&IS, BITS Pilani KK Birla Goa Campus, India

DANDAS@GOA.BITS-PILANI.AC.IN

Archana Mathur

Nitte Meenakshi Insitute of Technology, Yelahanka, Bangalore, India

MATHURARCHANA77@GMAIL.COM

Snehanshu Saha

APPCAIR and CS&IS, BITS Pilani KK Birla Goa Campus, India

SNEHANSHUS@GOA.BITS-PILANI.AC.IN

Abstract

Stochastic Gradient Descent (SGD) is the main approach to optimizing neural networks. Several generalization properties of deep networks, such as convergence to a flatter minima, are believed to arise from SGD. This article explores the *causality aspect of gradient descent*. Specifically, we show that the gradient descent procedure has an implicit granger-causal relationship between the reduction in loss and a change in parameters. By suitable modifications, we make this causal relationship explicit.

A causal approach to gradient descent has many significant applications which allow greater control. In this article, we illustrate the significance of the causal approach using the application of *Pruning*.

The causal approach to pruning has several interesting properties - (i) We observe a phase shift as the percentage of pruned parameters increase. Such phase shift is indicative of an optimal pruning strategy. (ii) After pruning, we see that minima becomes “flatter”, explaining the increase in accuracy after pruning weights.

Keywords: Granger Causality, Gradient Descent, Pruning Neural Networks

1. Introduction

Stochastic Gradient Descent (SGD) is the standard optimization procedure for deep neural networks. However, it surprised the researchers that SGD obtains solutions which generalize well. Several explanations such as sharp vs flat minima are given as evidence that the generalizability of deep networks is primarily due to properties of SGD (Neyshabur et al., 2017; Zhu et al., 2019). In this article we explore the *implicit causality in gradient descent procedure*.

Remark: Throughout the article we use the word causality to refer to Granger-type causality and not causality in the sense of graphical models.

The working hypothesis here is that – Gradient descent implicitly (and inefficiently) performs causal reasoning. And, by making the causal relationship explicit one can obtain a refined model of learning. We evidence the above hypothesis by applying this idea to pruning. We observe that removing the *non-causal* parameters almost always improves the accuracy and results in a much flatter minima.

Implicit causality in gradient descent: Note that every step of gradient descent results in a change of both the parameters θ and the loss function L . The change in parameters is dictated by the gradient of the loss function $\partial L/\partial\theta$. The implicit causality within this model is that - Changing $\theta \rightarrow \theta + \Delta\theta$ is expected to change the loss $L \rightarrow L + \Delta L$, where ΔL and $\Delta\theta$ are related by the first-order gradient information. In other words, “*changing the parameters θ causes the change in the loss*”. This however is not always true - there usually are parameters which do not result in the reduction in the loss. Thus, the implicit causality in the gradient descent is not perfect. We make the causality relationship explicit in section 2.

1.1. Application to Pruning

Making the causal relationship explicit can have several advantages. In this article we illustrate the advantage of this model for pruning.

Related Literature on Pruning: Pruning neural networks has gathered a lot of attention for variety of reasons - (i) Improves the efficiency of models at inference without compromising the accuracy (Kalchbrenner et al., 2018; Hoefler et al., 2021), (ii) Lottery ticket hypothesis (LTH) (Frankle and Carbin, 2019; Jin et al., 2022; Paul et al., 2023) and related works show that pruning experiments can help us understand the working of optimization and generalization in the training of neural networks. Two broad approaches for pruning are: (i) **Magnitude Based Pruning:** The popular heuristic that, the magnitude of the parameter reflects the importance of the weight, underlies several existing pruning methods. (Han et al., 2016; Gordon et al., 2020; Wang et al., 2023). In fact, as Wang et al. (2023) notes, using magnitude-based pruning at the level of filters (a.k.a L_1 norm pruning), the authors could achieve state-of-the-art results with this simple heuristic. (ii) **Impact Based Pruning:** Several pruning methods (LeCun et al., 1989; Singh and Alistarh, 2020) measure the dip in the loss function with respect to the parameters and decide which parameters to prune. Approaches such as one proposed by Singh and Alistarh (2020) use second-order Taylor approximation for the criterion. Benbaki et al. (2023) uses combinatorial optimization and approximates the Hessian using a low-rank matrix.

Causal vs Magnitude Pruning – Key results: In this article, we prune the parameters which turn out to be non-causal and hence refer to this procedure as *causal pruning*. As evidence to our hypothesis, we indeed observe that causal pruning finds a better optimal subset than the competitive methods such as magnitude pruning. Below we summarize the key results of which provides evidence to this claim. The details of the algorithm are delegated to the later sections.

The common approach to validate the pruning procedure is to observe the drop in test accuracy with respect to pruning percentage and measure the computation requirement using metrics such as FLOP count, etc. While these measures are suited for gauging the suitability of pruned network, they do not measure the optimality of the pruning procedure. We use two tests in this article, apart from test accuracy, to analyze optimality of the pruning procedure.

Test 1: A Phase Shift when plotting accuracy vs. pruning percent It is known that there exists a trade-off between accuracy and percentage pruned. If a pruning procedure is optimal in perfectly identifying the subset of “unimportant” parameters, we expect a sharp decrease in accuracy, even with a small change in percentage pruned. However, we see a smoother transition if the approximation of the subset is sub-optimal. Figure 1(a) shows a comparison of iterative versions of magnitude pruning and causal pruning. Intuitively, one does not expect much pruning in small networks (less

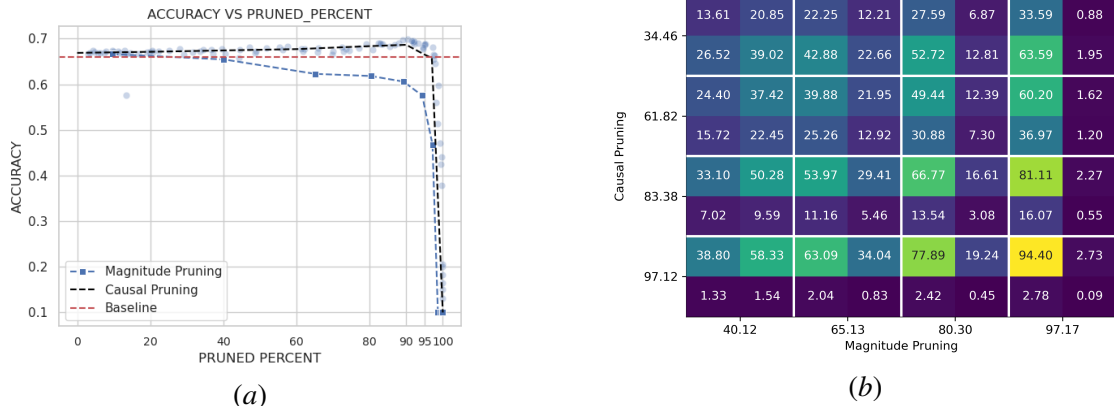


Figure 1: (a) Experiment on over-parameterized LeNet on CIFAR10 (*Top-Right is better*). There exists an accuracy-percent_pruned trade-off in general. Causal pruning achieves a much sharper transition than magnitude pruning. This evidences that causal pruning identifies better weights to prune than magnitude pruning. (b) Comparing Masks of Causal Pruning vs Magnitude Pruning. We compare 4 different masks of causal pruning with 4 different masks of magnitude pruning. In each 2x2 matrix, - (0,0) entry shows the percentage of intersection between the masks, (1,0) entry shows % of elements in magnitude pruning but not causal pruning, (0,1) entry shows the % of elements in causal pruning but not magnitude pruning, and (1,1) entry shows the number of elements not pruned by either. Observe that there is a decent overlap between the causal pruning masks and magnitude pruning masks. The values on the axes show the total % pruned. The results presented in (a), together with those in (b), indicate that while magnitude pruning is a strong heuristic, it fails to consistently identify the optimal set.

than 1M parameters). Here we consider a slightly over-parameterized LeNet (with 657,080 parameters) on the CIFAR10 dataset. Observe that the causal pruning reaches very close to the top-right corner, where removing even $\approx 2\%$ (going from 96% to 98% pruned_percent) more parameters results in a significant drop in accuracy. Contrast this with magnitude pruning, where the drop is much “smoother”. Thus this provides evidence that causal pruning can identify the parameters to be pruned much better than the magnitude heuristic.

Figure 1(b) compares the masks obtained by magnitude and causal pruning. Observe a decent overlap between the masks obtained by magnitude and causal pruning, indicating a strong correlation. However, at lower values of % pruned, the two methods diverge. The interesting case to consider is when both magnitude and causal pruning prune $\approx 97.1\%$ of the weights, the overlap is 94.4%. However, causal pruning attains an accuracy of 68.11% while magnitude pruning attains 46.8%. Surprisingly, these masks only differ by 2.7% of the weights. This shows that even minor differences in the weights pruned can lead to substantially different results.

Test 2: Flatter Minima It is widely believed that sharp minima lead to bad generalization and flat minima lead to better generalization (Jiang et al., 2020). If the pruning procedure is optimal, i.e., it reduces the number of parameters without affecting the accuracy, the model complexity is expected to reduce and we expect a flatter minima. Moreover, this also explains why few pruning

methods seem to *increase* the accuracy. We see that causal pruning obtains a much flatter minima than magnitude pruning. This is discussed in detail in section 4.

2. Causality and Gradient Descent

Notation: Let $p_{data} = \{x_i, y_i\}$ denote the dataset. Let f_θ denote the network to be trained. Let $L(\theta)$ denote the loss function used to optimize θ using Stochastic Gradient Descent (SGD). We use $\partial L(\theta^t)/\partial\theta$ to denote the derivative of L with respect to θ at $\theta = \theta^t$.

Let $\theta^0, \theta^1, \dots, \theta^t, \dots$ denote the path in the parameter space taken by the gradient descent. Further, we let

$$(\Delta L)^t = L(\theta^t) - L(\theta^{t-1}) \quad (1)$$

Let θ_i^t denote the i^{th} parameter in the vector θ^t . Then, we denote,

$$(\Delta\theta_k)^t = \theta_k^t - \theta_k^{t-1} \quad (2)$$

Vanilla Gradient Descent: We have,

$$\theta^{t+1} = \theta^t - \eta \frac{\partial L(\theta^t)}{\partial\theta} \quad (3)$$

where η denotes a fixed learning rate. Now, using a first-order Taylor approximation of L , we have

$$\begin{aligned} L(\theta^{t+1}) &= L\left(\theta^t - \eta \frac{\partial L(\theta^t)}{\partial\theta}\right) \\ &= L(\theta^t) - \eta \left(\frac{\partial L(\theta^t)}{\partial\theta}\right)^T \frac{\partial L(\theta^t)}{\partial\theta} \end{aligned} \quad (4)$$

Substituting from equation 3,

$$\begin{aligned} L(\theta^{t+1}) &= L(\theta^t) - \eta \left(\frac{\theta^t - \theta^{t+1}}{\eta}\right)^T \left(\frac{\theta^t - \theta^{t+1}}{\eta}\right) \\ &= L(\theta^t) - \frac{1}{\eta} \|\theta^t - \theta^{t+1}\|^2 \\ &= L(\theta^t) - \frac{1}{\eta} \sum_k (\theta_k^t - \theta_k^{t+1})^2 \end{aligned} \quad (5)$$

Granger Causal Interpretation: equation 5 can be interpreted as a specific case of vector-based Granger causality where the time-lag is considered to be 1 when written as below:

$$L^{t+1} = L^t + \sum_k \gamma_k (\theta_k^{t+1} - \theta_k^t)^2 \quad (6)$$

where $\gamma_k = -1/\eta$ for all k . In words, equation 5 can be interpreted as – “*Changing the parameter value by $\Delta\theta$ would cause the loss to reduce by the value ΔL .*” Nevertheless, this is not true in general. The loss does not reduce by ΔL but rather reduces by an unknown quantity. So, while the gradient descent assumes *implicit causal relationship* between the parameters and the loss reduction, it does not verify it nor does it adjust accordingly. In what follows we shall make this implicit causal relation explicit.

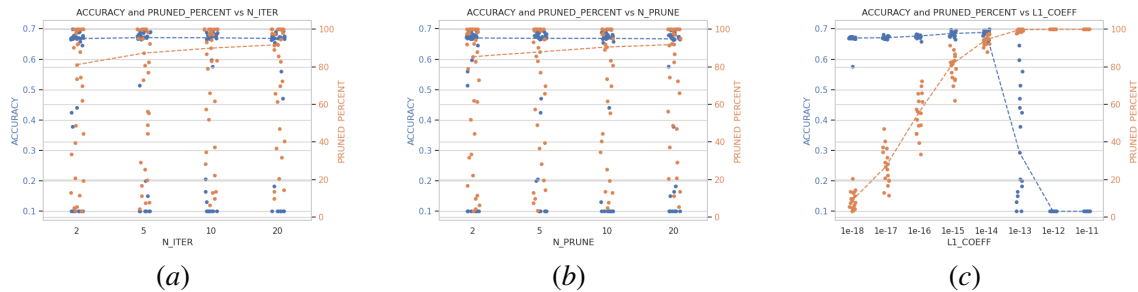


Figure 2: Effect of hyperparameters N_{iter} , N_{prune} and $L1_coeff$. These experiments have been performed using LeNet on CIFAR10. The dotted lines indicate the median percentage pruned and accuracy for each value. Observe that accuracy remains robust to the changes in N_{iter} and N_{prune} , while percentage pruned increases as N_{iter} and N_{prune} increase. We suggest default values of $N_{iter} = 10$ and $N_{prune} = 10$ as a balance between the computational complexity and pruning efficiency. $L1_coeff$ is the most important parameter which decides the percentage pruned. Interestingly, we observe that adding more parameters decreases the accuracy. This is explained by the observation that causal pruning reaches a much flatter minima than the unpruned version.

Remark: Note that we have only considered vanilla gradient descent above. Extending this analysis to SGD+momentum approaches and possibly SGD+momentum+adaptive-learning rates will result in a more comprehensive granger-causal model. A brief discussion of this can be found in appendix A. In this article, we are only interested in the model for vanilla gradient descent.

Making causal relation explicit by replacing $1/\eta$ with γ_k : Now generalizing from equation 5, assuming that each θ_k^t does not contribute equally to the reduction in the loss, we propose the following linear model which captures the dynamics of gradient descent -

$$\Delta L = \sum_k \gamma_k (\Delta \theta_k)^2 \quad (7)$$

Here γ_k denotes the importance of parameter θ_k . This is in line with the Granger-causal interpretation above.

By replacing the constant learning rate across all parameters with parameter specific γ_k , we are able to capture information that is not possible to measure otherwise. As we shall exhibit in this article, this information is crucial for identifying the importance of a parameter. Specifically, we have the following principle – *Consider the parameter θ_k to be important if $\gamma_k \neq 0$, and unimportant if $\gamma_k = 0$.*

3. Causal Pruning Algorithm

Pruning as Feature Selection: From equation 7, we have a linear model with features/independent variables $\{(\Delta \theta_k)^2\}$ with coefficients γ_k and dependent variable ΔL . Thus, selecting the parameters is the same as testing $H_0 : \gamma_k = 0$ vs $H_1 : \gamma_k \neq 0$. In other words, selecting a subset of parameters (a.k.a pruning) is the same as finding the subset of features in the above linear model. This matches the Granger-causal interpretation of causal parameters as well. A vast amount of literature from

Table 1: List of parameters

Name	Explanation	Typical Values
N_{pre}	Number of epochs for training the network after which the pruning is performed	5-10
N_{iter}	Number of iterations of pruning to be performed	2-10
N_{prune}	Number of epochs for training the network to collect the data required for causal pruning	2-10
N_{post}	Number of epochs for training the network after pruning to evaluate the performance	100-300
L1_coeff	The regularization parameter used for LassoRegression	1e-18 to 1e-11 (log space)

Algorithm 1 Causal Pruning

-
- 1: **Parameters:** $N_{pre}, N_{iter}, N_{prune}, N_{post}, \text{L1_coeff}$. (See table 1 for details).
 - 2: **Input:** Model: f_θ , Dataset: $\{\mathbf{x}_i, y_i\}$
 - 3: Train the model for N_{pre} number of epochs.
 - 4: **for** $i = 1, 2, \dots, N_{iter}$ **do**
 - 5: Train the model for N_{prune} epochs and collect the values of the parameters and the losses after each gradient step. Let $\{(\theta^t, L^t)\}$ denote the values after each gradient step.
 - 6: For each layer, using Lasso Regression, fit the model in equation 7 using the L_1 coefficient L1_coeff. Prune the parameters for which $\gamma_k = 0$.
 - 7: Reset the remaining weights to be the ones after step 3.
 - 8: **end for**
 - 9: Complete the training of the model for N_{post} number of parameters.
-

classical statistics (James et al., 2023) deals with this problem. We use a sparse solution based on L_1 regularization for subset selection.

Pretraining: Given a dataset and architecture, we train the model for N_{pre} epochs. This is crucial as pointed out by Blalock et al. (2020). This phase decides the *basin of attraction* of the parameters after which the model can be pruned more effectively.

Causal Pruning: After the pretraining, we have the pruning phase. Here, we further train the model for N_{prune} epochs and collect the parameters and losses after each gradient step. Let $\{\theta^t, L^t\}_{t=0}^T$ denote the values we obtain. Starting at $t = 1$, compute first-order differences,

$$\begin{aligned}\Delta\theta^t &= \theta^t - \theta^{t-1} \\ \Delta L^t &= L^t - L^{t-1}\end{aligned}\tag{8}$$

and fit the model using $\{\Delta\theta^t, \Delta L^t\}_{t=1}^T$ as the dataset. Here $\Delta\theta$ denotes the independent variables and ΔL denotes the dependent variables.

$$\Delta L = \sum_k \gamma_k (\Delta\theta_k)^2 + \alpha \sum_k |\gamma_k|\tag{9}$$

where α denotes the L_1 regularization coefficient. We obtain the pruning masks as $\{\theta_k \mid \gamma_k \neq 0\}$. Repeat this process N_{iter} times to get the final mask. After each pruning step, we *rewind* the weights to the weights obtained after pretraining. This allows for pruning a larger subset of weights.

Post Training: To maximize the performance of the network, we train it further (using only unpruned weights) for N_{post} number of epochs.

Important Remarks:

Optimization of equation 9: For some networks, the number of parameters within each layer can go up to $16M$ and hence can cause memory issues. Shalev-Shwartz and Tewari (2011) discusses several algorithms for stochastic optimization of equation 9. We follow the procedure outlined in (Tsuruoka et al., 2009). We also further restrict the feature (parameter) selection with each layer, i.e. solve equation 9 for each layer separately.

Computational Complexity: Apart from the usual training of the networks, this procedure requires two additional steps - (i) Saving the checkpoints of the model after each gradient step for a few epochs, and (ii) Solving the lasso regression of the equation 9. Note that saving the checkpoints does not increase the computational complexity, but does require a larger storage. Further, these checkpoints can be removed after the computation of the coefficients in equation 9. Solving equation 9 is a straightforward problem and there exist several efficient solutions which use stochastic gradients (Shalev-Shwartz and Tewari, 2011; Tsuruoka et al., 2009). The naive approach has the computational complexity of $\mathcal{O}(mdk)$ where m is the number of samples, d is the number of features and k is the number of epochs required to reach the solution. Note that it scales linearly in both the number of samples and some parameters (features), and hence very efficient. Further, these algorithms can also be parallelized, leading to higher gains.

Parameter-Level or Layer-Level or Entire-Network: It sometimes helps to prune channels or layers instead of individual parameters. This is referred to as structured pruning (He and Xiao, 2024). One can adapt the procedure in equation 7 to structured pruning using the strategy of *weight-sharing*. In essence, enforce the constraint that γ_k is equal for all parameters θ_k within a layer. In this article, we only consider Parameter-Level pruning a.k.a unstructured pruning.

Difference from existing Magnitude/Impact based pruning: The proposed pruning method is substantially different from existing approaches (see section 1). Magnitude-based pruning methods rely heavily on the magnitude heuristic, while we consider the gradient descent dynamics. Impact-based pruning methods estimate the dip in the loss with respect to each parameter, which is used for pruning. However, we on the other hand compare the predicted dip in the loss with the actual dip in the loss and use this for defining and pruning unimportant parameters.

4. Experiments and Analysis:

Scope of Experiments: Recall that the key idea in this article is to make explicit the implicit causal relation within gradient descent. We consider the application of pruning to explore the power of this observation. Our focus is not on achieving state-of-the-art results but on substantiating the claim above. Specifically, causal pruning prunes an *optimal* subset compared to the magnitude heuristic as a baseline. The code for these experiments can be found at <https://anonymous.open.science/r/causalpruning-9DB5/README.md>

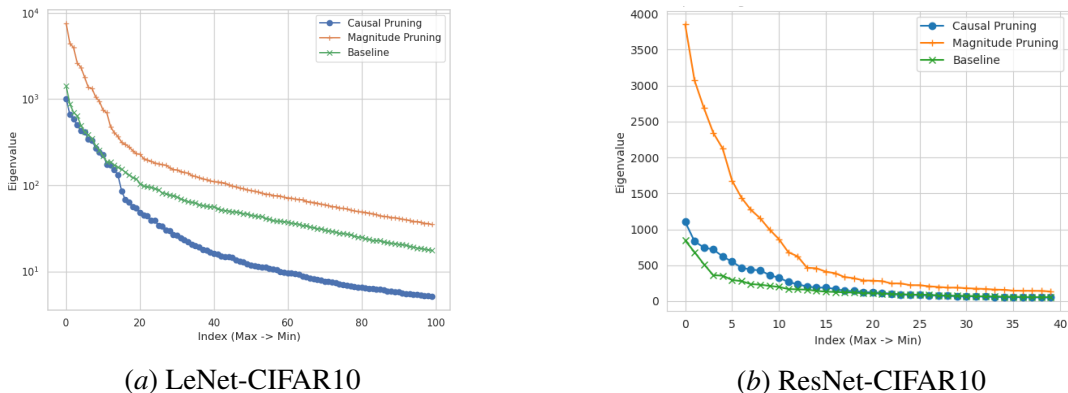


Figure 3: Top Eigenvalues at minima of various pruning methods. Understanding the flatness of the minima is the key to understanding the generalization of neural networks. With the “right” pruning approach we expect to see a flatter minima comparable to the original network. As shown in the plots, magnitude pruning tends to increase the eigenvalues (leading to sharper minima) compared to causal pruning (which gives flatter minima).

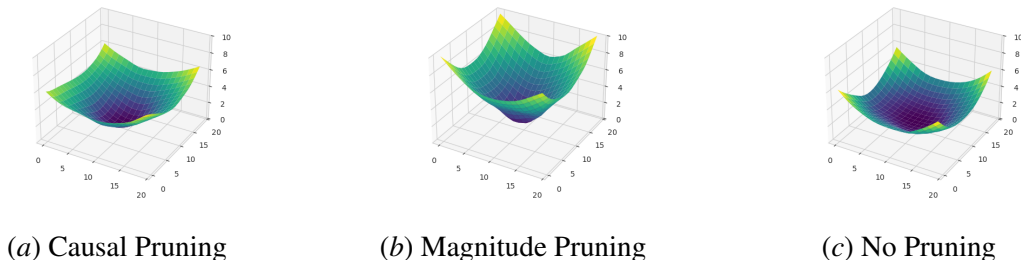


Figure 4: Loss Landscape of ResNet18 on CIFAR10 for various pruning strategies. As one can see, causal pruning obtains a flatter minima close to the original network, while magnitude pruning increases the sharpness of the minima. This is another piece of evidence to support that - While magnitude pruning is a strong heuristic, it does prune a few “important” parameters. Figure 5 in the appendix shows the corresponding plots for LeNet on CIFAR10.

4.1. Dependence on the Hyperparameters

The parameters required for causal pruning are shown in table 1. We consider N_{pre} large enough that the SGD is within a basin of attraction, and N_{post} large enough that there is no further improvement to the loss function. Hence, we only consider N_{iter} , N_{prune} and $L1_coeff$. Figure 2 shows the accuracy and percentage pruned for various values of the parameters. These studies have been done using LeNet on the CIFAR10 dataset.

Accuracy of Causal pruning is fairly robust to N_{iter} and N_{prune} : Figure 2(a) shows the stripplot for various values of N_{iter} and figure 2(b) shows the stripplot for N_{prune} . Recall that N_{iter} denotes the number of times we repeat the pruning procedure, and N_{prune} indicates the number of epochs we train the network to collect the data used for fitting equation 9. The dotted lines indicate the median percentage pruned and accuracy for each value.

Table 2: Comparing Causal Pruning with Magnitude pruning. The results are presented as percent-pruned (test accuracy).

Model (# Params)	Dataset	No-Pruning	Magnitude Pruning	Causal Pruning
LeNet (657,080)	FashionMNIST	0.0%(90.51%)	65.13%(90.31%)	68.72%(90.39%)
	CIFAR10	0.0%(64.49%)	95.99%(55.71%)	96.30%(67.22%)
	TinyImageNet	0.0%(17.79%)	95.99%(9.93%)	96.08%(19.49%)
AlexNet (57,044,810)	FashionMNIST	0.0%(91.05%)	95.99%(91.09%)	93.37%(91.25%)
	CIFAR10	0.0%(70.29%)	95.99%(69.88%)	99.13%(72.01%)
	TinyImageNet	0.0%(37.38%)	88.71%(41.89%)	88.72%(41.64%)
ResNet18 (11M)	FashionMNIST	0.0%(92.79%)	85.22%(92.08%)	85.21%(92.32%)
	CIFAR10	0.0%(74.05%)	91.11%(76.18%)	91.17%(78.45%)
	TinyImageNet	0.0%(29.40%)	77.87%(28.22%)	73.93%(29.72%)

Observe that the accuracy is unaffected at different values of N_{iter} and N_{prune} . Again, this can be explained as the manifestation of our hypothesis that causal pruning identifies the important weights precisely. If this had not been the case, we expect changes in accuracy when changing the number of pruning steps. However, the percentage pruned increases nominally and we increase the values of N_{iter} and N_{prune} . Increasing the values N_{prune} and N_{iter} from 10 to 20 improves the results nominally but at $2\times$ the cost. Hence, we consider 10 the default value for these hyperparameters.

Effect of L1_coeff: `L1_coeff` is arguably the most important hyper-parameter which directly controls the sparsity. Figure 2(c) shows the changes in accuracy and `percent_pruned` by changes in `L1_coeff`. Concerning `pruning_percent`, we observe the expected trend - as `L1_coeff` increases, the percentage pruned also increases. This is expected since the `L1_coeff` directly affects the number of 0s in the solution of equation 9, which in turn is used to prune the parameters.

However, the interesting thing to note is the change in accuracy. Observe that at `L1_coeff = 1e-14` (68.8%) has a (slightly) larger accuracy than `L1_coeff = 1e-18` (66.9%). This is because causal pruning obtains a flatter minima than the unpruned model. Hence, adding the parameters leads to noise that results in slightly lesser accuracy. Also, as observed earlier, there is a sharp increase in the accuracy as `L1_coeff` changes from $1e-12$ to $1e-14$.

An important deviation of causal pruning from the existing approaches is that we do not control the amount of pruning. Rather, we let the model decide the amount to be pruned based on the `L1_coeff`.

4.2. Causal Pruning Obtains a Flatter Minima

Review of Flat Minima vs Generalization: One popular hypothesis to explain the generalization of deep neural networks is the ideas of *flat minima*. Putting this simply, when the minima are flatter, one expects to see better generalization. Jiang et al. (2020) performs extensive experiments and shows that the *sharpness of the minima* is the most correlated measure with generalization. Foret et al. (2021) proposes a sharpness-aware minimization optimizer, which is shown to have better

results than the rest of the minima. [Ahn et al. \(2024\)](#) uses the trace of the Hessian normalized by the dimension to measure the sharpness of the minima.

Flat Minima in the context of Pruning: Another way to judge if a particular subset of parameters is the “right” subset to prune is that *It should result in a flatter minima comparable to the original network*. The intuition behind this is, that as we reduce the number of parameters, the complexity of the model reduces, hence the minima should be flatter leading to a better/comparable generalization. Note that the flat minima perspective also explains why one sees a slight improvement in test accuracy with mild pruning.

Figure 3 shows the top eigenvalues obtained with different pruning strategies for ResNet18 and LeNet on CIFAR10. We observe that causal pruning either improves (in the sense of flatter minima) the eigenspectrum of the Hessian or remains the same as the no-prune network. In contrast, magnitude pruning increases the eigenvalue spectrum by a large margin. Figure 4 visualizes the loss landscape of the minima obtained for ResNet18 on CIFAR10. Figure 5 (supplementary material) shows the corresponding plots for LeNet on CIFAR10. Details of these experiments and approaches used to generate these plots are discussed in appendix B.

Comparison on other dataset/model combinations: Table 2 shows the results across various dataset/model combinations. We consider 3 architectures - LeNet ([LeCun et al., 1998](#)), Alexnet ([Krizhevsky et al., 2012](#)) and ResNet18 ([He et al., 2016](#)), and 3 different datasets - FashionMNIST ([Xiao et al., 2017](#)), CIFAR10 ([Krizhevsky, 2009](#)) and TinyImageNet ([Le and Yang, 2015](#)). Note that we outperform magnitude pruning in almost all these settings. As stated before, this is attributed to the ability of causal pruning to capture the dynamics of gradient descent.

Comparison with CHITA ([Benbaki et al., 2023](#)): While our primary goal is not to achieve state-of-the-art results, we present a comparison with the current leading method, CHITA, to provide a comprehensive perspective. Using ResNet50 on the ImageNet dataset for all experiments, we observe notable differences in performance within the context of single-shot pruning. Our causal pruning approach achieves an accuracy of 71%¹ with 80% pruning, compared to CHITA’s approximate 45% with 80% pruning². However, when employing gradual pruning (specifically, two pruning steps in our causal pruning process), our method reaches 56% accuracy at 95% pruning, whereas [Benbaki et al. \(2023\)](#) reports a 73% accuracy at 95% pruning.

It’s important to note that our objectives differ significantly; we focus on understanding the intricacies and artifacts of pruning, whereas [Benbaki et al. \(2023\)](#) is geared towards optimizing pruning for speed and state-of-the-art performance. Additionally, these comparisons are observational, conducted without hyper-parameter tuning, and the computational setups³ involved vary significantly.

5. Conclusion and Future Work

In conclusion, the key idea in this article is to re-interpret gradient descent from the perspective of causality. Specifically, we make the Granger-causal perspective explicit by suitably modifying the gradient descent. This allows for a different framework for optimizing deep networks. We explored the application of pruning in this article.

1. 54% after pruning and 71% after fine-tuning

2. These figures are derived from Figure 2(a) in ([Benbaki et al., 2023](#)) based on observation

3. CHITA uses a batch size of 5000 and uses approx. 200 CPUs and 10 GPUs, while we perform the experiments on 40 CPUs and 4 GPUs.

Causality and Pruning: On pruning, the following are the key takeaways from this article:

- When making the causal relationship explicit, we observe that each parameter is mapped to a γ_k , which holds a piece of important information. Specifically, whether a parameter is important or not can be decided by testing whether $\gamma_k = 0$ vs $\gamma_k \neq 0$. That is, by testing whether the corresponding θ_k is causal or not. Thus, we refer to this technique as *causal pruning*.
- To implement causal pruning, we frame the problem of testing causality as a lasso regression problem. Thanks to the vast literature on lasso regression, this can be implemented very efficiently.
- *Judging if a specific subset of parameters are the right parameters to be pruned?* Traditionally test accuracy has been the approach to validate whether a pruning procedure is optimal. In this article, we propose and use 2 more validation techniques
 - **Phase Shift Validation:** The pruning procedure should result in a *phase-shift* when plotting accuracy vs percent_pruned. The sharper the transition, the better the method. Intuitively this is because, if there exists a perfect subset of parameters for pruning, then pruning any more parameters above this should reduce the accuracy drastically.
 - **Flat Minima Validation:** An optimal pruning procedure should not increase the sharpness of minima. Specifically, it should not increase the large eigenvalues leading to a different output from the original unpruned network. Moreover, this also explains why few pruning approaches tend to increase test accuracy.
- We show that causal pruning is better than the currently widely used approach of magnitude pruning on all these measures.

Extensions to Causal Pruning: There are several possible extensions to the present work (i) In this article we focus on unstructured pruning. However, a simple extension to structured pruning is possible by using a weight-sharing strategy in equation 9, where the lasso coefficients are shared as per the structure. For instance, let θ_k denote each parameter and γ_k represent the corresponding lasso coefficient. To prune entire layers/filters, ensure that $\gamma_i = \gamma_j$ for any parameters θ_i and θ_j that belong to the same layer/filter. This uniformity ensures that parameters within a single layer are treated equivalently during the pruning process. (ii) One can extend the lasso model in equation 9 to SGD with momentum and even to SGD with momentum and adaptive learning rates. This is briefly discussed in the supplementary material (appendix A). (iii) In the current manuscript, we have performed a layer-wise optimization of equation 9. We intend to extend this to a single optimization for the entire network, from which we expect modest gains.

Other Applications of Causal Interpretation: We envision several other applications to the causal perspective of gradient descent.

- *Causal Second Order Optimization:* A slightly different interpretation of the causal pruning presented in this article is – We perform *two first-order optimizations which can encapsulate second-order information*. Specifically, we perform one first-order optimization on reducing the loss, and the second first-order optimization based on the explainability (causality) of

parameters to the reduction of the loss. This, in effect, is equivalent to the second-order optimization method. Specifically, we believe that the parameters γ_k obtained as causal pruning are related to the “optimal” parameter-specific learning rate of the first-order optimization. We aim to explore this as part of the future work.

- *Increasing the capacity of the network using causality:* Note that pruning is aimed at reducing the size of the model for efficient inference. However, a significant drawback of these approaches is that – Training still requires one to consider the entire model. And since training the model is arguably the costliest aspect, the impact of pruning on cost is rather small.

Instead, one can ask the question – *Can we start with a small model and increase its capacity at the time of optimization?* This article provides one approach to answer this question in the affirmative. Specifically, at the time of optimization, if a specific parameter turns out to be redundant, one can reinitialize the parameter, which increases the capacity. For such an approach to work, the criterion selected for pruning should be optimal – i.e. reduce both false positives and false negatives. As we show in this article, *causal pruning* satisfies this objective. Hence, as part of future work, we aim to explore this line of research as well.

Acknowledgments

Aditya Challa acknowledges the support from CEFIPRA(68T05-1). Snehanshu Saha and Aditya Challa would like to thank the Anuradha and Prashanth Palakurthi Center for Artificial Intelligence Research (APPCAIR) and SERB CRG-DST (CRG/2023/003210) for their support. Snehanshu Saha acknowledges SERB SURE-DST (SUR/2022/001965) and the DBT-Builder project (BT/INF/22/SP42543/2021), Govt. of India for partial support. Archana Mathur would like to thank SERB TARE (TAR/2021/000206) for their support

References

- Kwangjun Ahn, Ali Jadbabaie, and Suvrit Sra. How to escape sharp minima with random perturbations. In *Int. Conf. Mach. Learning*, 2024.
- Riade Benbaki, Wenyu Chen, Xiang Meng, Hussein Hazimeh, Natalia Ponomareva, Zhe Zhao, and Rahul Mazumder. Fast as CHITA: neural network pruning with combinatorial optimization. In *Int. Conf. Mach. Learning*, 2023.
- Davis W. Blalock, Jose Javier Gonzalez Ortiz, Jonathan Frankle, and John V. Guttag. What is the state of neural network pruning? In *Machine Learning and Systems*, 2020.
- Pierre Foret, Ariel Kleiner, Hossein Mobahi, and Behnam Neyshabur. Sharpness-aware minimization for efficiently improving generalization. In *Int. Conf. on Learning Representations*, 2021.
- Jonathan Frankle and Michael Carbin. The lottery ticket hypothesis: Finding sparse, trainable neural networks. In *Int. Conf. on Learning Representations*, 2019.
- Mitchell A. Gordon, Kevin Duh, and Nicholas Andrews. Compressing BERT: studying the effects of weight pruning on transfer learning. In *RepLANLP@ACL*, 2020.

- Song Han, Huizi Mao, and William J. Dally. Deep compression: Compressing deep neural network with pruning, trained quantization and huffman coding. In *Int. Conf. on Learning Representations*, 2016.
- Kaiming He, Xiangyu Zhang, Shaoqing Ren, and Jian Sun. Deep residual learning for image recognition. In *Proc. Conf. Comput. Vision Pattern Recognition*, 2016.
- Yang He and Lingao Xiao. Structured pruning for deep convolutional neural networks: A survey. *IEEE Trans. Pattern Anal. Mach. Intell.*, 2024.
- Geoffrey Hinton, Nitish Srivastava, and Kevin Swersky. Rmsprop, 2014. https://www.cs.toronto.edu/~tijmen/csc321/slides/lecture_slides_lec6.pdf.
- Torsten Hoefler, Dan Alistarh, Tal Ben-Nun, Nikoli Dryden, and Alexandra Peste. Sparsity in deep learning: Pruning and growth for efficient inference and training in neural networks. *J. Mach. Learning Research*, 2021.
- Gareth James, Daniela Witten, Trevor Hastie, Robert Tibshirani, and Jonathan Taylor. *An Introduction to Statistical Learning: with Applications in Python*. Springer International Publishing, 2023. ISBN 9783031387470. doi: 10.1007/978-3-031-38747-0.
- Yiding Jiang, Behnam Neyshabur, Hossein Mobahi, Dilip Krishnan, and Samy Bengio. Fantastic generalization measures and where to find them. In *Int. Conf. on Learning Representations*, 2020.
- Tian Jin, Michael Carbin, Daniel M. Roy, Jonathan Frankle, and Gintare Karolina Dziugaite. Pruning’s effect on generalization through the lens of training and regularization. In *Neural Inform. Process. Syst.*, 2022.
- Nal Kalchbrenner, Erich Elsen, Karen Simonyan, Seb Noury, Norman Casagrande, Edward Lockhart, Florian Stimberg, Aäron van den Oord, Sander Dieleman, and Koray Kavukcuoglu. Efficient neural audio synthesis. In *Int. Conf. Mach. Learning*, 2018.
- Diederik P. Kingma and Jimmy Ba. Adam: A method for stochastic optimization. In *Int. Conf. on Learning Representations*, 2015.
- Alex Krizhevsky. Learning multiple layers of features from tiny images, 2009. URL <https://www.cs.toronto.edu/~kriz/learning-features-2009-TR.pdf>.
- Alex Krizhevsky, Ilya Sutskever, and Geoffrey E. Hinton. Imagenet classification with deep convolutional neural networks. In *Neural Inform. Process. Syst.*, 2012.
- Ya Le and Xuan Yang. Tiny imagenet visual recognition challenge, 2015. Stanford University.
- Yann LeCun, John S. Denker, and Sara A. Solla. Optimal brain damage. In *Neural Inform. Process. Syst.*, 1989.
- Yann LeCun, Léon Bottou, Yoshua Bengio, and Patrick Haffner. Gradient-based learning applied to document recognition. *Proc. IEEE*, 1998.
- Hao Li, Zheng Xu, Gavin Taylor, Christoph Studer, and Tom Goldstein. Visualizing the loss landscape of neural nets. In *Neural Inform. Process. Syst.*, 2018.

- Ilya Loshchilov and Frank Hutter. SGDR: stochastic gradient descent with warm restarts. In *Int. Conf. on Learning Representations*, 2017.
- Behnam Neyshabur, Srinadh Bhojanapalli, David McAllester, and Nati Srebro. Exploring generalization in deep learning. In *Neural Inform. Process. Syst.*, 2017.
- Mansheej Paul, Feng Chen, Brett W. Larsen, Jonathan Frankle, Surya Ganguli, and Gintare Karolina Dziugaite. Unmasking the lottery ticket hypothesis: What’s encoded in a winning ticket’s mask? In *Int. Conf. on Learning Representations*, 2023.
- Shai Shalev-Shwartz and Ambuj Tewari. Stochastic methods for l_1 -regularized loss minimization. *J. Mach. Learning Research*, 2011.
- Sidak Pal Singh and Dan Alistarh. Woodfisher: Efficient second-order approximation for neural network compression. In *Neural Inform. Process. Syst.*, 2020.
- Yoshimasa Tsuruoka, Jun’ichi Tsujii, and Sophia Ananiadou. Stochastic gradient descent training for l_1 -regularized log-linear models with cumulative penalty. In *Int. Joint Conf. on Natural Language Processing ACL-AFNLP*, 2009.
- Huan Wang, Can Qin, Yue Bai, and Yun Fu. Why is the state of neural network pruning so confusing? on the fairness, comparison setup, and trainability in network pruning. *arXiv:2301.05219*, 2023.
- Han Xiao, Kashif Rasul, and Roland Vollgraf. Fashion-mnist: a novel image dataset for benchmarking machine learning algorithms. *arXiv:1708.07747*, 2017.
- Zhewei Yao, Amir Gholami, Kurt Keutzer, and Michael W. Mahoney. Pyhessian: Neural networks through the lens of the hessian. In *IEEE Int. Conf. on Big Data*, 2020.
- Zhanxing Zhu, Jingfeng Wu, Bing Yu, Lei Wu, and Jinwen Ma. The anisotropic noise in stochastic gradient descent: Its behavior of escaping from sharp minima and regularization effects. In *Int. Conf. Mach. Learning*, 2019.

Appendix A. Deriving the Causal Relation in the case of SGD + Momentum

Let’s consider the following variant of the gradient descent with momentum-

$$\begin{aligned} v^{t+1} &= \beta v^t + \frac{\partial L(\theta^t)}{\partial \theta} \\ \theta^{t+1} &= \theta^t - \eta v^{t+1} \end{aligned} \tag{10}$$

where β denotes the momentum hyperparameter. Then, we have, using first-order Taylor approximation,

$$\begin{aligned} L(\theta^{t+1}) &= L(\theta^t) - \eta \left(\frac{\partial L(\theta^t)}{\partial \theta} \right)^T v^{t+1} \\ &= L(\theta^t) - \eta \beta \left(\frac{\partial L(\theta^t)}{\partial \theta} \right)^T v^t - \eta \left(\frac{\partial L(\theta^t)}{\partial \theta} \right)^T \frac{\partial L(\theta^t)}{\partial \theta} \end{aligned} \tag{11}$$

Now from equation 10 using previous time steps, we can derive

$$v^t = \frac{\theta^t - \theta^{t-1}}{\eta} = \frac{\Delta\theta^t}{\eta} \quad (12)$$

and,

$$\frac{\partial L(\theta^t)}{\partial \theta} = -\frac{v^{t+1} - \beta v^t}{\eta} = -\frac{\Delta\theta^{t+1} - \beta\Delta\theta^t}{\eta^2} \quad (13)$$

Substituting, equation 12 and equation 13 in equation 11, we get,

$$L(\theta^{t+1}) - L(\theta^t) = -\eta\beta \left(-\frac{\Delta\theta^{t+1} - \beta\Delta\theta^t}{\eta^2} \right)^T (\Delta\theta)^t - \eta \left\| -\frac{\Delta\theta^{t+1} - \beta\Delta\theta^t}{\eta^2} \right\|^2 \quad (14)$$

Ignoring the constants β, η , and replacing them with c_1, c_2, c_3 ,

$$(\Delta L)^{t+1} = c_1 \|\Delta\theta^{t+1}\|^2 + c_2 \|\Delta\theta^t\|^2 + c_3 (\Delta\theta^t)^T \Delta\theta^{t+1} \quad (15)$$

where c_1, c_2, c_3 are some fixed functions of η, β . Using the same principle above, and replacing the coefficients with parameter specific γ_k . However, note that here we have three possibly independent features for each parameter θ_k - Time difference at $t = t_0$, Time difference at $t = t_1$, and the cross feature between the differences. Hence instead of using a single parameter γ_k (as in the case of vanilla gradient descent), one needs to use $(\gamma_{k,0}, \gamma_{k,1}, \gamma_{k,2})$. The model then becomes,

$$(\Delta L)^{t+1} = \sum_k \gamma_{k,0} (\Delta\theta_k^{t+1})^2 + \gamma_{k,1} (\Delta\theta_k^t)^2 + \gamma_{k,2} (\Delta\theta_k^t) (\Delta\theta_k^{t+1}) \quad (16)$$

Here we consider the parameter to be not-important if $\gamma_{k,0} = \gamma_{k,1} = \gamma_{k,2} = 0$, i.e all the coefficients should be irrelevant.

We also replace the causal pruning step, with the following - Starting at $t = 2$, compute first-order differences,

$$\begin{aligned} \Delta\theta^{t,0} &= \theta^t - \theta^{t-1} \\ \Delta\theta^{t,1} &= \theta^{t-1} - \theta^{t-2} \\ \Delta L^t &= L^t - L^{t-1} \end{aligned} \quad (17)$$

and fit the model using $\{\Delta\theta^{t,0}, \Delta\theta^{t,1}, \Delta L^t\}_{t=1}^T$ as the dataset. Here $\Delta\theta^0, \Delta\theta^1$ denotes the independent variables and ΔL denotes the dependent variables.

$$\Delta L = \sum_k \gamma_{k,0} (\Delta\theta_k^0)^2 + \gamma_{k,1} (\Delta\theta_k^1)^2 + \gamma_{k,2} (\Delta\theta_k^0) (\Delta\theta_k^1) + \alpha \sum_k (|\gamma_{k,0}| + |\gamma_{k,1}| + |\gamma_{k,2}|) \quad (18)$$

We obtain the pruning masks as,

$$\{\theta_k \mid \gamma_{k,0} \neq 0 \text{ or } \gamma_{k,1} \neq 0 \text{ or } \gamma_{k,2} \neq 0\} \quad (19)$$

Remark: What about the case with varying learning rates? It turns out that it is not easy to adapt the above procedure to gradient descent with adaptive learning rates such as ADAM (Kingma and Ba, 2015) or RMSProp (Hinton et al., 2014). Specifically, one would have to consider all the significant updates till time t - $\{\Delta\theta^t\}_{t=0}^{t=t}$. Since this is computationally expensive and also since it is known that SGD with momentum works sufficiently well in practice (Loshchilov and Hutter, 2017), we do not consider this case in the current scope of the article.

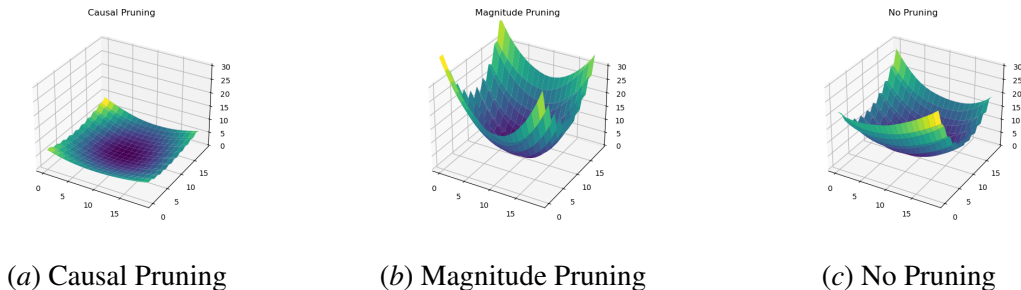


Figure 5: Loss Landscape

Appendix B. Details of Flat Minima Experiments

To obtain the top eigenvalues from trained networks, we use the stochastic power-iteration method from Yao et al. (2020). For visualizing the minima, we use the method proposed in Li et al. (2018), which is the following:

1. We consider two arbitrary directions by initializing a network with weights from a normal distribution with mean 0 and standard deviation 1 - u_1 and u_2 . We then normalize the filters to have the same norm as the original network

$$u_{i,j} = \frac{u_{i,j}}{\|u_{i,j}\|} \|d_{i,j}\| \quad (20)$$

where $u_{i,j}$ refers to the j^{th} filter from i^{th} layer of randomly initialized network, and $d_{i,j}$ refers to the j^{th} filter from i^{th} layer of the trained network.

2. We then plot the loss obtained by $f(\theta^* + \alpha u_1 + \beta u_2)$ where f refers to the network architecture, θ^* refers to the parameters of the original network and $\alpha, \beta \in (-1, 1)$. This is visualized as a 3d plot as shown in the figures. Further, we also scale the z-axis as $\log(1 + f(\theta))$ for better visualization.

Appendix C. Experimental Setup

All experiments were carried out on an NVIDIA DGX V100 server. The server is equipped with an Intel(R) Xeon(R) CPU E5-2698 v4 CPU with 20 physical cores running 40 threads, paired with 256 GB of system memory. The server also houses four NVIDIA Tesla-V100-DGXS GPUs, each possessing 32GB of VRAM.

We used Adam optimizer for prepruning training and post-pruning training steps with a learning rate of $5e-4$. We used the SGD optimizer with a learning rate of $1e-3$ for the pruning steps. Models were trained until the training loss stopped decreasing beyond the minimum training loss achieved for at least 5 epochs where the current training loss would be considered worse than the best training loss if it didn't improve upon the best loss by more than $1e-4$. We took the best model measured by accuracy on the validation set to report the results.

We used $N_{pre} = 10$, $N_{iter} = 10$, $N_{prune} = 10$, and $N_{post} = 200$ unless specified otherwise. We used $batch_size = 512$ except for ResNet50 where we used $batch_size = 256$ to make the model fit in VRAM.

Table 3: Hyperparameters used to run experiments

Model	Dataset	L1_coeff	mag_prune_frac
LeNet	FashionMNIST	1e-14	0.1
	CIFAR10	1e-14	0.275
	TinyImageNet	1e-14	0.275
AlexNet	FashionMNIST	1e-17	0.275
	CIFAR10	1e-16	0.275
	TinyImageNet	1e-16	0.196
ResNet18	FashionMNIST	1e-16	0.174
	CIFAR10	1e-15	0.215
	TinyImageNet	1e-15	0.14

Table 3 shows the `L1_coeff` and `mag_prune_frac` used for experiments reported in this paper. `L1_coeff` controls the amount of Causal Pruning in each pruning iteration. `mag_prune_frac` is the fraction of global params pruned in every pruning iteration of Magnitude Pruning. We chose specific `mag_prune_frac` to match the final prune percentage obtained by Causal Pruning.